KfK 4034
Januar 1986

Jet Fragmentation

G. Flügge
Institut für Kernphysik

Kernforschungszentrum Karlsruhe

KERNFORSCHUNGSZENTRUM KARLSRUHE

Institut für Kernphysik

KfK 4034

JET FRAGMENTATION

Günter Flügge

Kernforschungszentrum Karlsruhe GmbH, Karlsruhe

Jet Fragmentation

ABSTRACT

Data on jet fragmentation, in particular recent results from e^+e^- and $\bar{p}p$ collisions, are presented in the framework of phenomenological models. The Lund string model and the Webber QCD cluster model turn out to describe the data quite well. Shortcomings of both models are discussed.

Jet Fragmentation

ZUSAMMENFASSUNG

Daten über Jet-Fragmentation, insbesondere neue Ergebnisse von e^+e^- und $\bar{p}p$ Reaktionen, werden im Rahmen phänomenologischer Modelle vorgestellt. Das Lund-'string'-Modell und das Webber-QCD-Schauer-Modell beschreiben die Daten recht gut. Unzulänglichkeiten beider Modelle werden diskutiert.

Invited talk at "The Quark Structure of Matter" Conference, Strasbourg - Karlsruhe, 26. September - 1 Oktober 1985

CONTENT:

1. INTRODUCTION

Since jets had first been seen in pp[1] and e^+e^- [2] reactions about 10 years ago, a wealth of data on this phenomenon has been collected at e^+e^- machines, in lepton-nucleon scattering and at pp and $\bar{p}p$ colliders. Most of the information in this report comes from the study of e^+e^- annihilation at CESR, DORIS, PEP, and PETRA and from very new data obtained at the S$\bar{p}$pS collider. Recent reviews of the subject have been given at Bari[3] and Kyoto[4].

Hadronic jets occur in pp, $\bar{p}p$, lN and e^+e^- reactions as the result of hard scattering processes as shown in Fig. 1. The quark and gluon jets which are seen in the different processes are of course only comparable if factorization of the three components of the processes is fulfilled:

a) structure functions describing the incoming partons
b) hard scattering processes
c) fragmentation of the outgoing quarks and gluons

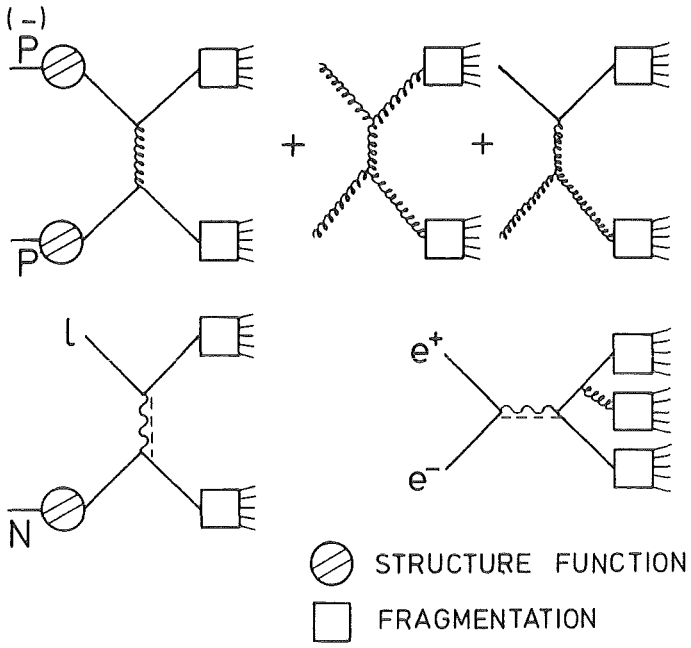

Fig. 1: Jet production in $\overset{(-)}{p}p$, ℓp and e^+e^- reactions.

This factorization of soft a) and c) and hard b) processes has recently been shown to hold in the framework of QCD[5] up to logarithmic terms which can be absorbed in scaling violation terms of a) and c).

Contrary to the hard process b) which can be calculated in perturbative QCD, we do do not have the mathematical tools (yet) to calculate the soft processes a) and c) in QCD. We are therefore forced to use models.

After a short introduction of the functions used to describe fragmentation and a brief discussion of some basic features (multiplicities) of hadronic jets I will therefore first introduce the most important models of fragmentation and then discuss the detailed measurements in the framework of these models.

a) Fragmentation Function

Fragmentation functions are most easily introduced in the reaction

$$e^+e^- \rightarrow q\bar{q} \rightarrow \text{hadrons} \qquad (1)$$

where no structure functions are involved.

The cross section is simply given by

$$\frac{d\sigma}{dx} = \sigma_{q\bar{q}} \cdot 2 \cdot D_q^h(x,Q^2) = \frac{8\pi\alpha^2}{s} Q_q^2 D_q^h(x,Q^2) \qquad (2)$$

(s = (cm energy)^2, Q^2 = (momentum transfer)^2, Q_q = quark charge).

$D_q^h \stackrel{!}{=} D_{\bar{q}}^h$ is called the fragmentation function. Two different parameters are used for the scaling variable x:

$$x = \frac{E_h}{E_b} \quad \text{or} \quad x_p \equiv z = \frac{p_h}{p_b} \qquad (3)$$

where E_h, E_b, p_h, p_b are the hadron or beam energy or momentum. Since $\beta \frac{d\sigma}{dx} = \frac{d\sigma}{dz}$ the scale invariant cross sections for the two variables read

$$\frac{s}{\beta}\frac{d\sigma}{dx} \sim D_q^h(x) \quad \text{or} \quad s\frac{d\sigma}{dz} \sim D_q^h(z) \qquad (4)$$

Depending on the measured quantities both distributions are used and both should scale (be independent of Q^2) in the simple quark parton model (QPM).

Fig. 2 shows this approximate scaling in the case of reaction (1) for $x_p > 0.2$. [6] At low x, the scaling violation is attributed to quark thresholds.

b) Multiplicities

In the simple quark parton model one would expect a logarithmic increase of the multiplicity. However, at large energies the mean charged multiplicity deviates from the QPM prediction by about one unit in $\langle n_{ch} \rangle$. This can be explained by scaling violation due to gluon bremsstrahlung (Fig. 3).

In the case of hadron collisions, the picture is more complicated. Whereas low energy pp data from the ISR are rather close to the e^+e^- jet multiplicities the high energy $\bar{p}p$ jet multiplicities are higher, somewhere between the quark and gluon jet prediction: [7]

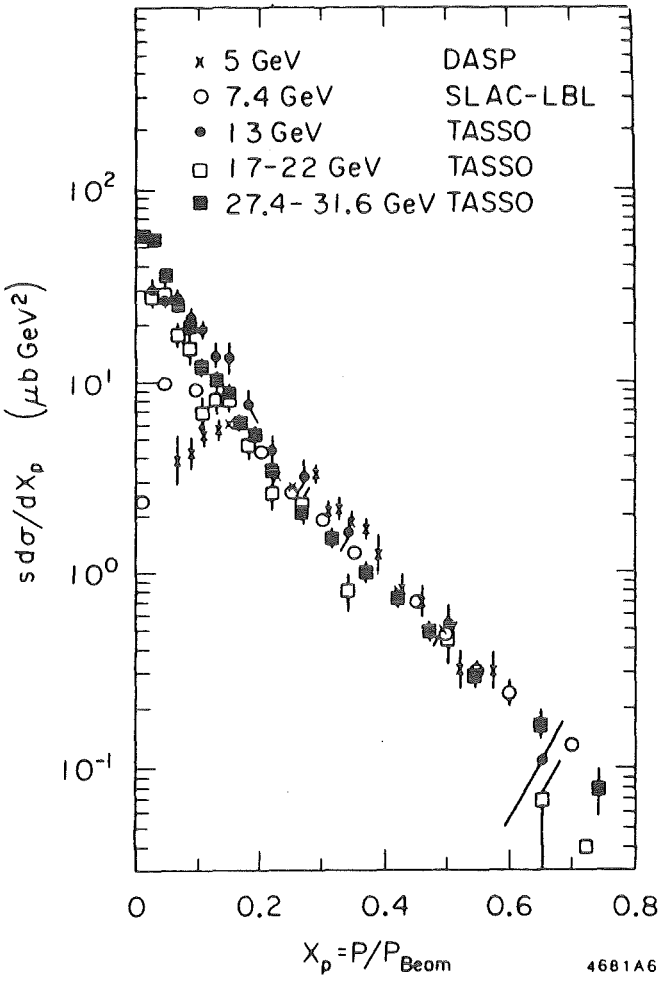

Fig. 2:
Inclusive hadron cross section in e^+e^- annihilation for a wide range of energies.

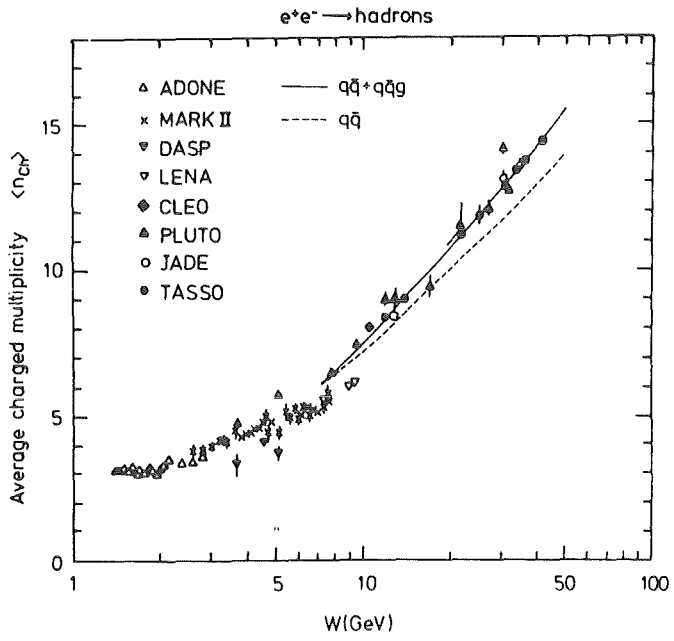

Fig. 3:
Mean charged multiplicity in e^+e^- annihilation. The predictions are for the simple QPM and for QCD calculations including gluon-bremsstrahlung.

$$\frac{\langle n\rangle_g}{\langle n\rangle_q} = \frac{9}{4}\left\{1 - \frac{27+N_f}{27}\sqrt{\frac{\alpha_s}{6\pi}} - O(\alpha_s)\right\} \qquad (5)$$

(N_f = number of flavours, α_s = strong coupling constant).

This is not unexpected since at high energies a large fraction of the $\bar{p}p$ jets are of gluonic origin (c.f. chapter 5b). However, given the difficulties of defining jet multiplicities in proton collisions one certainly needs more data to draw definite conclusions.

New data from the EMC collaboration[8] indicate that $\langle n_{ch}\rangle$ not only depends on $\sqrt{s}$ but also on Q^2. The slight increase of $\langle n_{ch}\rangle$ with Q^2 can be attributed to gluon bremsstrahlung and is consistent with QCD expectations with (Fig. 4)

$$\Lambda = 480 \begin{smallmatrix} + 270 \\ - 230 \end{smallmatrix} \text{ MeV}.$$

Also KNO scaling has been tested in e^+e^- [6] μp [8] and $(\bar{p})p$ [9] scattering. The approximate scaling found at intermediate energies in all three types of reactions is strongly violated at the high $\bar{p}p$ energies[9].

Multiplicities between the two jets in reaction (1) are essentially uncorrelated as expected in the simple QPM picture[10),11]

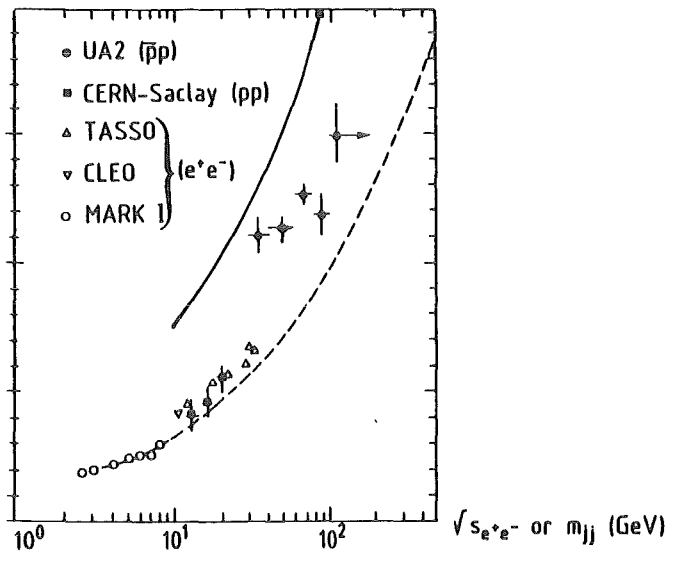

Fig. 4:
Mean charged multiplicity per jet as a function of the two-jet mass m_{jj}. e^+e^- data are compared with $\bar{p}p$ and pp data. The curves show the extrapolation of the e^+e^- data (quark jets, dashed line) and the prediction for gluon jets (full line).

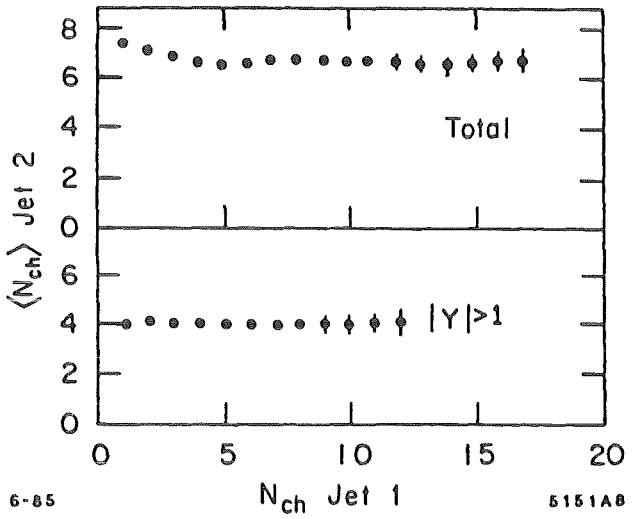

Fig. 5:
Charged multiplicity (n_{ch}) correlations
a) Mean charged multiplicity $\langle n_{ch} \rangle$ of one jet as a function of n_{ch} of the other jet in e^+e^- annihilation.

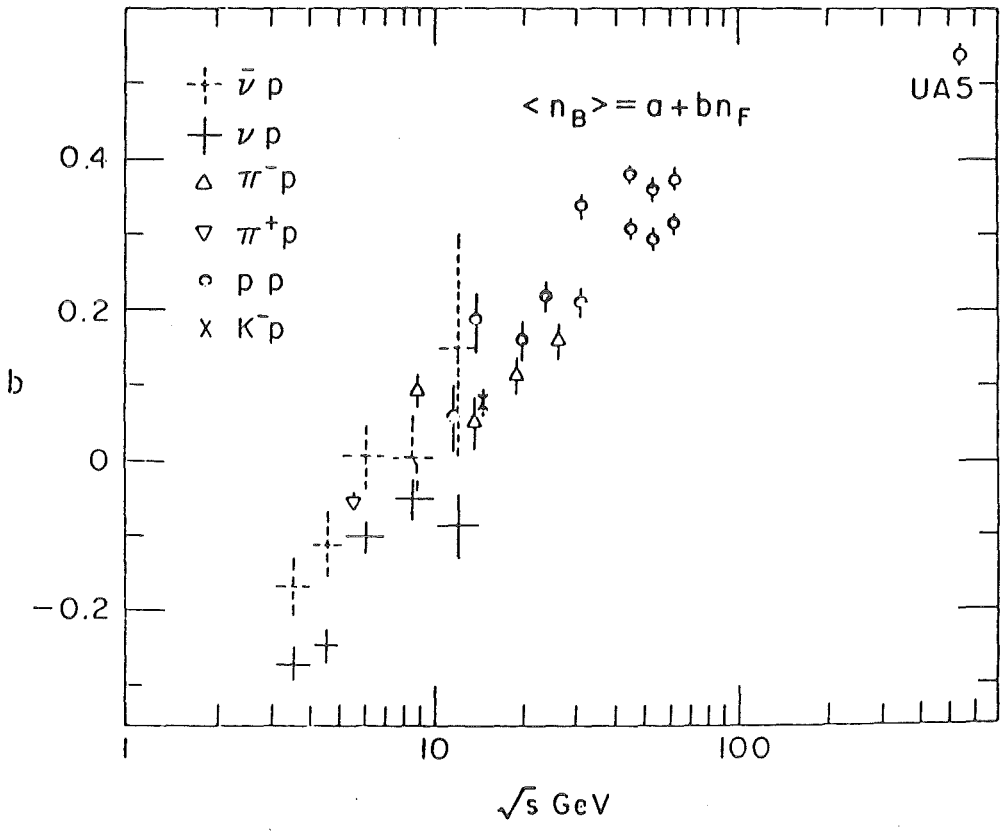

Fig. 5b) Forward-backward correlations for lepton-proton and hadronic reactions.

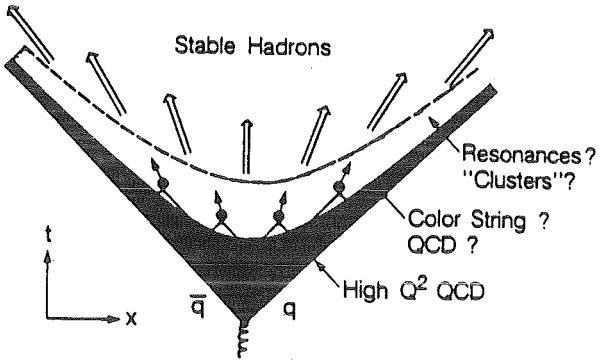

Fig. 6:
Fragmentation of a $\bar{q}q$ pair produced in e^+e^- annihilation.

(Fig. 5a). The same is true for jets in lepton proton collisions. In contrast to this a rather strong forward-backward jet correlation[12] is seen in $\overset{(-)}{p}p$ collisions (Fig. 5b). This indicates that the underlying (soft hadron) physics in these processes is quite different, even if gross features sometimes look quite similar like in the case of jet multiplicities or KNO scaling.

2. FRAGMENTATION MODELS

Since no final theory of jet fragmentation is available yet, we have to rely on models to keep track of the large amount of data available in this field.

The basic ingredients of these models are presented[13] in Fig. 6 for the case of reaction (1): the $q\bar{q}$ pair looses its high virtuel mass in some kind of gluon-quark cascade. At the end of this process quarks and gluons materialize into primordial hadrons which eventually decay into the stable hadrons seen in the detector.

There are basically two classes of models to describe this process:

I. Perturbative QCD + Phenomenology

The first few steps of the cascade are calculated exactly in first or second order perturbative QCD. All the rest is described by phenomenological models, which divide class I into two types:

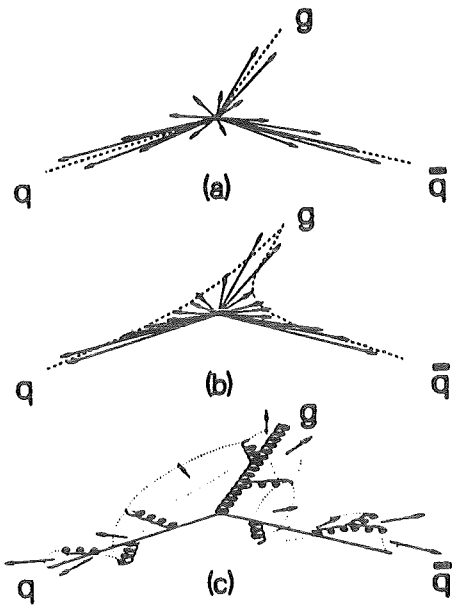

Fig. 7:
Three types of fragmentation models[4]

a) Independent Fragmentation (IF)

b) String Fragmentation (SF)

c) QCD Cluster Models (CF)

Independent Fragmentation Models (IF)

Quarks and gluons produced in perturbative QCD fragment independently[14] (Fig. 7a). Fragmentation functions, transverse momenta, heavy quark suppression etc. are put in by hand.

String Fragmentation Models (SF)

The two quarks traveling apart loose energy in a linear confining potential producing a color string of tension $k \approx 1$ GeV/fm. If the separation in proper time $\tau = \Delta x^2 - \Delta t^2$ is larger than m^2/k^2 $q\bar{q}$ pairs of mass m will be formed and the process will be iterated until all energy is used up. Transverse momentum and high mass suppression are built in quite naturally by a "tunneling" process in the $q\bar{q}$ pair creation[15),16),17)]. Important for the distinction between different models is the treatment of gluons as transverse excitations of the string (Fig. 7b).

In practice, both the IF and SF have in common a large number of free parameters and functions like

- fragmentation function D(z)

- mean transverse momentum
- quark flavour ratio u:d:s
- vector/pseudoscalar ratio V/PS
- baryon production
- heavy quark production.

Although, contrary to the IF the treatment and magnitude of many of these parameters is well motivated in the SF, they finally enter as free parameters in the comparison to real data.

II. QCD shower models

A quite different approach is persued in the QCD shower models[18]. Most of the QCD cascade is calculated in leading log approximation and only the last step of the hadronisation is made by a phenomenological model (Fig. 7c).

Gottschalk Model[19]

The QCD cascade is terminated when the virtuality of the partons has reached a cutoff value Q_o. The cascade is controlled by Altarelli-Parisi splitting functions and the QCD scale parameter Λ. In a preconfinement stage colourless clusters (or strings for $M \geq M_f$) are formed which decay according to phase space and known decay properties of resonances.

Webber Model[20]

Whereas only colinear singularities are considered in the Gottschalk model also soft singularities are taken into account in the Webber model. This results in an angular ordering of subsequent branchings in the cascade

$$\theta_{k+1} < \theta_k$$

which leads to similar distinctive features as the SF model (c.f. chapter 5a).

Let me stress again that contrary to the models of type I, the QCD shower models II make do with three parameters only, Λ, Q_o and M_f.

In the following, data will be compared mainly to the two most successfull models, the Lund (SF) and the Webber model. The other two models will be shown to fail fatally in chapter 5a.

3. LIGHT QUARK FRAGMENTATION

a) Particle Content of Jets

An impressive amount of inclusive particle data has been accumulated at e^+e^- storage rings in the energy range 10 GeV $\lesssim \sqrt{s} \lesssim$ 40 GeV. At least one member of most isospin multipletts in the pseudoscalar and vector meson octets and the baryon J = 1/2 octet and J = 3/2 decuplet has been measured[3,4]. In particular, new results on the decuplet were presented by the ARGUS group recently[21]. No data are available for η', ω and Σ. Also, unfortunately only upper limits exist so far for the Δ resonances.

A summary of mean particle multiplicities is given in Ref. 3 and 4. A comparison with fits to the Lund and Webber model in Ref. 4 shows that both models can account quite well for the data.

Also the measured differential cross sections are in general well reproduced by both models. A difficulty seems to exist however in the invariant Λ cross section[22]. The rapid fall off at $z \approx 0.2$ cannot be correctly described by the Lund model. Since most Λ's at small z come from charm and bottom baryon decays, the suspicion is that these particles are not correctly handled in the model.

The model parameters used to desribe the data and typical adjusted values are summarized in Table 1.

Given the large amount of data the successes of both models are quite impressive. The agreement with the Webber model is particularly remarkable in view of the few free parameters used. It seems to indicate that the hadronisation at $Q^2 \approx \Lambda^2$ is in fact dominated by phase

TABLE 1: Typical values used for the model parameters

Lund		Webber
$u\bar{u}$: $d\bar{d}$: $s\bar{s}$ = 1:1 : γ_s	$\gamma_s \approx 0.33$	Λ = 0.5 GeV
P / P + V	= 0.3 ÷ 0.5	Q_o = 0.6 GeV
$\frac{d\sigma}{dp_\perp^2} = \exp\left(-\frac{p_\perp^2}{2\sigma_q}\right)$	σ_q = 300 MeV	M_f = 4 GeV
$D(z) = z^{-1}(1-z)^{a_L}$	a_L = 0.5 ÷ 2	
Peterson function (see chapter 4)	$\varepsilon_c \approx 0.04$ $\varepsilon_b \approx 0.01$	
P(uu) : P(u)	= 0.08 ÷ 0.10	
$\frac{P(us)}{P(s)} : \frac{P(ud)}{P(d)}$	= 0.3 ÷ 0.7	

space. Of course this is a simplification which must have its limits.

These limitations of a cluster decay model become apparent in the leading particle (high z) distribution measured recently by the HRS group[22),4)]. Contrary to the Lund SF model the Webber cluster model fails to describe the inclusive charged particle cross section near $z \approx 1$.

In addition to the pseudoscalar and vector mesons and octet and decuplet baryons, the f^0 has been observed by the CLEO[25)] and the $\iota(1460)$ by the JADE[24)] group (3σ effect). Particularly interesting is also the production of antideuterons by the ARGUS group[23)]. 6 events have been detected by dE/dx, TOF and interaction in the detector wall. The rate of $\bar{d}/\pi$: $(\bar{p}/\pi)^2 \approx 2 \cdot 10^{-3}$ is similar to the relative rate at which $\bar{d}$ were seen in pN collisions before.

b) Particle Correlations

Long and Short Range Correlations

In reaction (1) some kind of memory of the $q\bar{q}$ origin of the two jets would lead to long range correlations LRC between the two jets. In addition, local conservation of charge, strangeness and baryon number would invoke short range correlations SRC (Fig. 8)[13),27),28)]. Two particle correlations have been studied by the TASSO[30)], PLUTO[31)], and TPC[32)] groups. The TPC result for π and K correlations are shown in Figs. 9 and 10. An associated opposite charge density is defined:

$$q_a^b(y) = \rho^{-a}_{b}(y) - \rho^{+a}_{b}(y) \qquad (6)$$

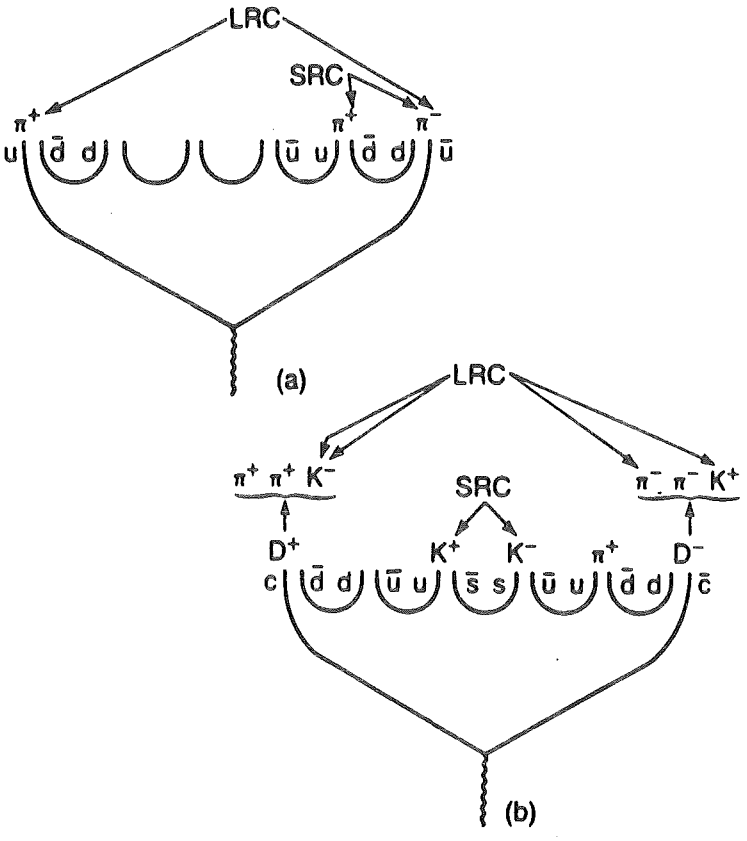

where ± a indicates the particle type b with same/opposite charge as a, with a,b either π or K and a the trigger particle. All $\pi\pi$, KK and πK correlations show clear SRC. If the trigger π is at low rapidity a strong SRC is seen due to resonance decay and presumably also local charge compensation in the hadronisation. If the trigger gap is moved to larger va-

Fig. 8: Mechanisms for long range and short range correlations in e^+e^- annihilation.

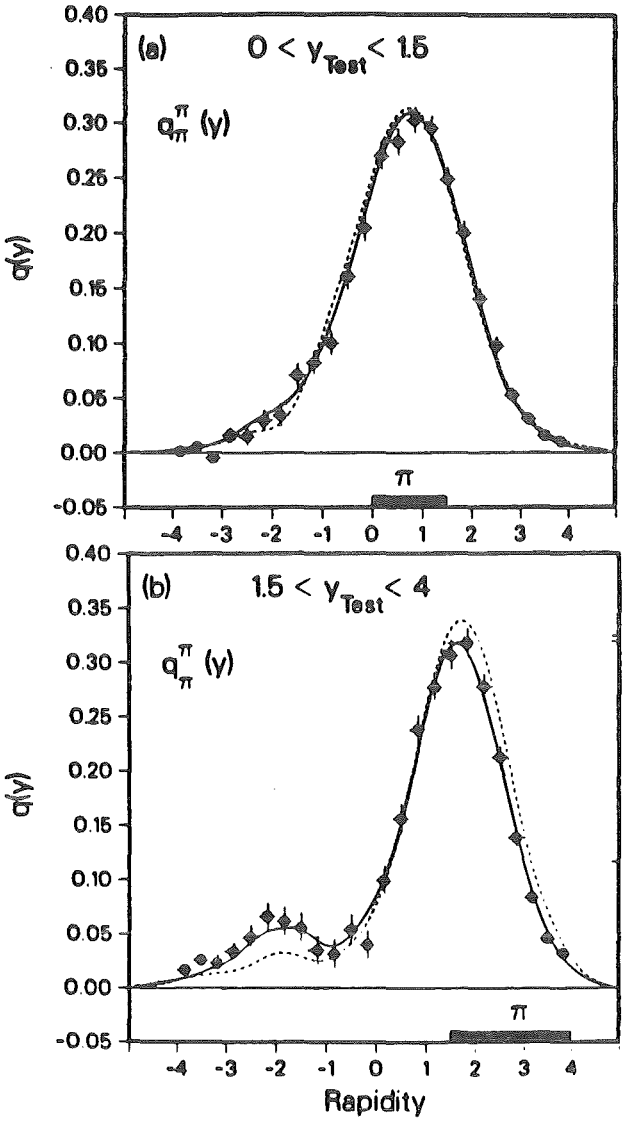

Fig. 9:
Associated opposite charge density as a function of rapidity for K and π in various combinations. The trigger rapidity range is shown as a thick bar
a)+b) ππ correlations for different trigger rapidity.

lues (Fig. 9b), additional LRC show up giving evidence for leading particle fragmentation of the primary partons. In the KK rapidity correlations of Fig. 10a the SRC and LRC are of similar size since resonance decay is quite unimportant in this case. This provides clear evidence for local charge compensation in the fragmentation cascade. The LRC is further evidence for a strong leading strange particle component containing primary strange quarks. Fig. 10b finally shows a clear anti LRC as expected from the decay of leading charm particles (c.f. Fig. 8).

Bose-Einstein-Correlations

Once pions and kaons are formed they will obey the rules of Bose-Einstein statistics for integer spin particles. Due to the symmetrisation of the wave function an enhancement at low relative Q^2 is

expected in the production of equal charge π's or K's (GGLP effect). The ratio of equal to opposite charge π's or K's

$$R_{BE} = \frac{N(++,--)}{N(+-,-+)} \sim 1 + \lambda \exp(-R_o^2 Q^2) \qquad (7)$$

is usually parametrized in terms of the incoherence λ and the source radius R_o. Recent evidence for such correlations has been seen by the MARK II[34], TPC[35], CLEO[36], and TASSO[30] groups in e^+e^- annihilation and by the AFS collaboration[37] at the ISR. The TASSO data are shown in Fig. 11. Their result is $R_o(2\pi) = (0.77 \pm 0.14)$ fm and $R_o(3\pi) = (0.48 \pm 0.11)$ fm in good agreement with the other e^+e^- results. The AFS group has determined $R_o(2K) = (2.4 \pm 0.9)$ fm (slightly different parametrisation).

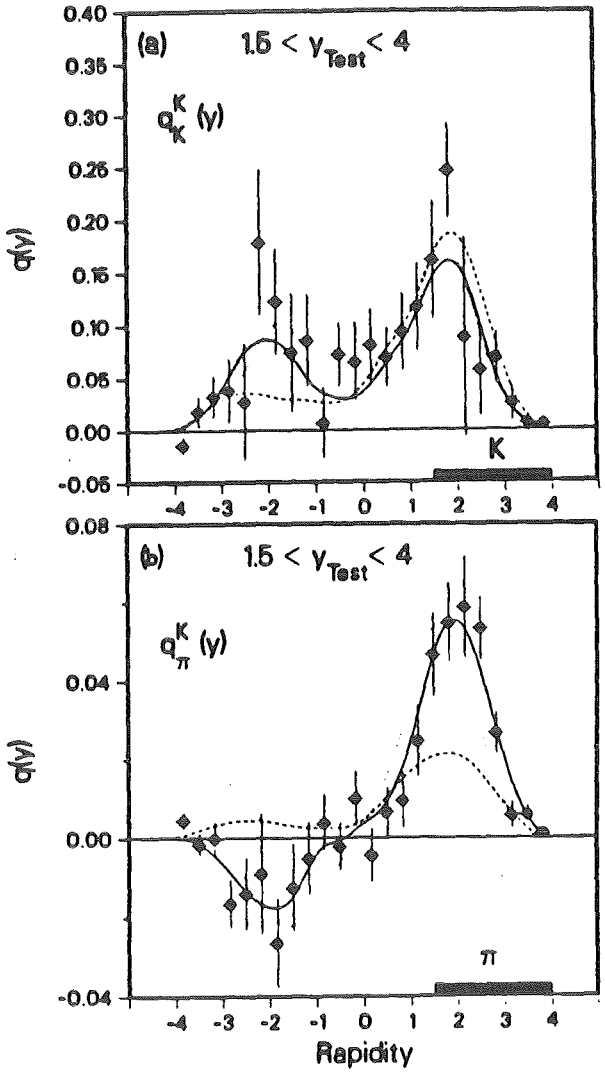

Fig. 10: As Fig. 9:
a) KK correlation,
b) Kπ correlation.

c) Baryon Production

Sizable baryon production seen in pp, μp and e^+e^- jets has stimulated many suggestions to explain the data[38]. The baryon production mechanism proposed are schematically summarized in Fig. 12:

a) Recombination Models[38),39)] (Fig. 12a):
Three quarks recombine sta-

tistically to form a pair of $B\bar{B}$. Tests: rapidly correlations and $p_\perp$ distributions.

b) Leading Diquark Model[40),41)] (Fig. 12b):

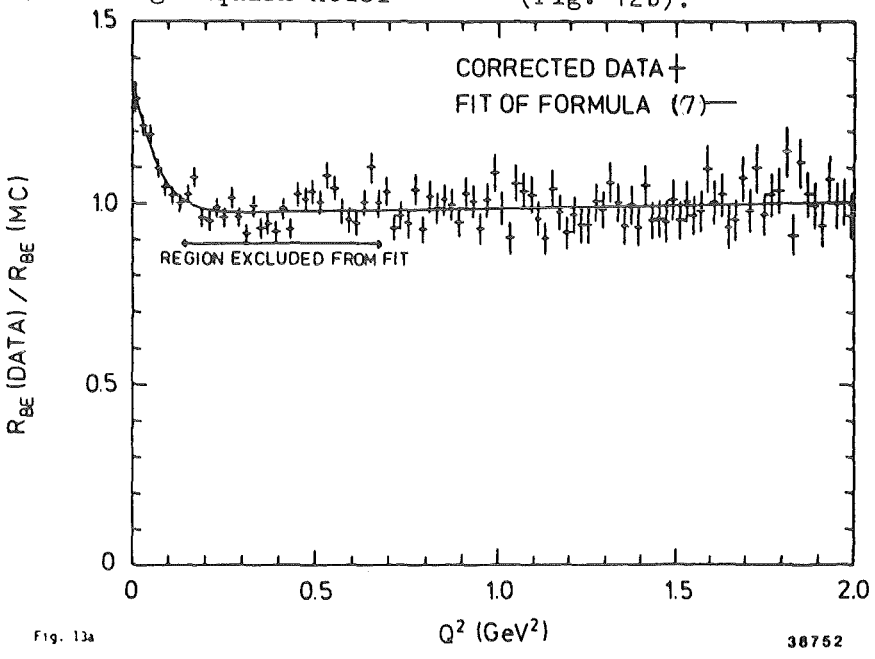

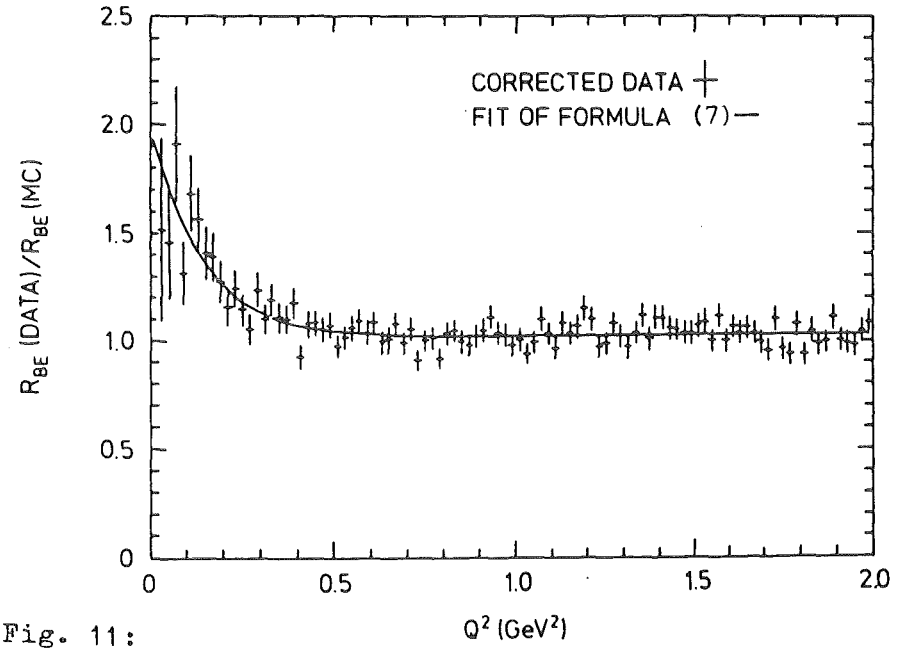

Fig. 11:
Bose-Einstein correlations for two (a) and three (b) pions with a fit to formula (7).

Diquarks are produced in the primary annihilation process.
Test: long range Correlations.

c) Diquark Production (refs. 40), 42),43)) (Fig. 12c): Diquarks-antidiquark pairs are produced ad hoc in the fragmentation process.
Test: $B\bar{B}$ rapidity correlation.

d) Pop Corn Model[44),45)] (Fig. 12d): Similar to model a) diquark-antidiquark pairs

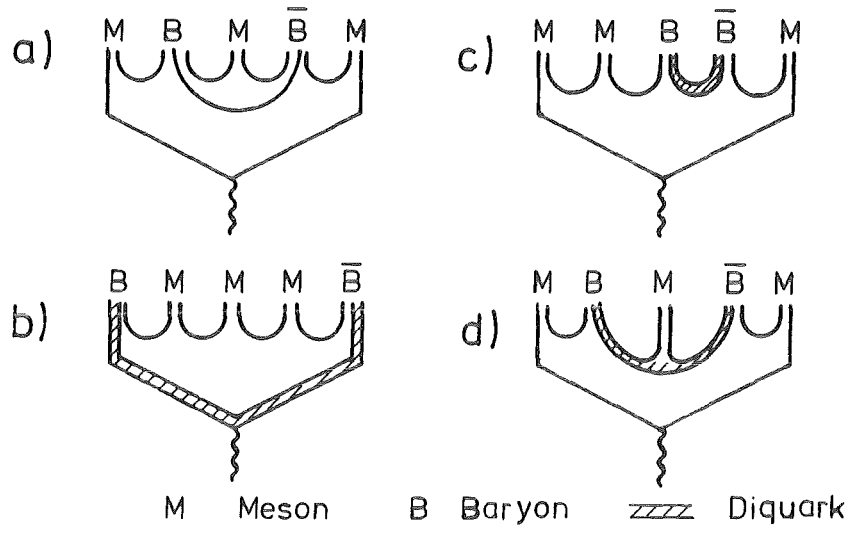

Fig. 12:
Baryon production mechanisms.

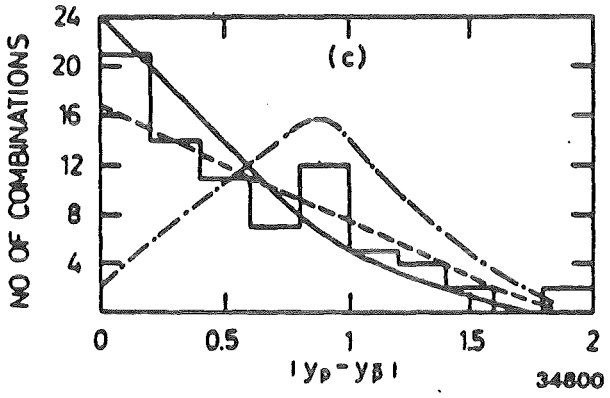

Fig. 13:
$p\bar{p}$ rapidity correlations compared to model predictions of models a) (-·-), b) in independent fragmentation (--), and c) in the Lund model (—).

produced by colour fluctuations in the $q\bar{q}$ string. The resulting model is intermediate between model a) and c). Test: $p_\perp$ and θ correlations of the $B\bar{B}$ system.

e) Cluster Decay Model[20),46)] (Fig. 7c): $q\bar{q}$ mesons decay into $B\bar{B}$. Test: angular distribution of the $B\bar{B}$ system wrt the jet axis.

Diquark vs. Single Quark

The decisive tests are rapidity correlations (Fig. 13) and $p_\perp$ distributions (Fig. 14). Recombination models fail to explain the SRC of the $\bar{p}p$ data which is well described by the diquark model[47)]. Also the $p_\perp$ distributions are in excellent agreement with diquark models, in which $\langle p_\perp \rangle_B \approx \sqrt{2}\,\langle p_\perp \rangle$. $\langle p_\perp \rangle_B \approx \sqrt{3}\,\langle p_\perp \rangle$ of model a) overestimates the measured $\langle p_\perp \rangle_B$ slightly[48)]. In both tests the diquark model is

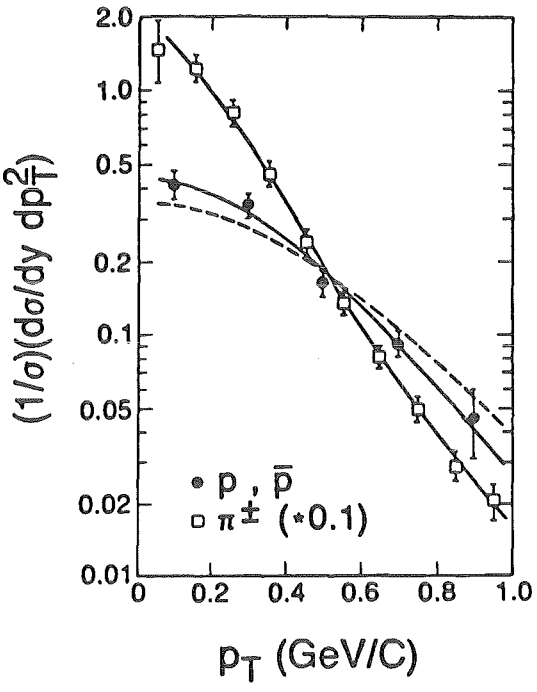

Fig. 14:
$p_\perp$ distributions of $p,\bar{p}$ compared to $\pi^\pm$. Data are confronted with models a) (--) and c) in the Lund model (—).

clearly favored. From LRC data[49] leading diquarks can be estimated to contribute < 15%.

Diquark vs. Cluster

In the $B\bar{B}$ rest frame the angular distribution of the $B\bar{B}$ production angle θ^* wrt the jet axis is expected to show distinct differences: in a cluster model e) the distribution will be flat in cos θ^* whereas it will be forward peaked in the diquark Lund model c) since the diquarks and thereby the $B\bar{B}$ will preferentially follow the string direction. Fig. 15 shows the TPC data for protons compared to the Lund and Webber model[50]. Whereas the Lund model is in excellent agreement with the data, the Webber model seems to be in trouble (TPC: Webber model excluded at 95% C.L.).

Diquarks vs. Pop corn

In a 'pure' diquark model c) the diquark pair production will lead to a strong back-to-back correlation of the baryons in the $B\bar{B}$ rest frame. No such correlation is expected in the 'popcorn' model d) because the two diquarks are separated in the fragmentation cascade. Recent studies of the TPC group show that at least 45% 'popcorn' is needed to describe the data (90% C.L.)[4),29)].

This result is corraborated by measurements of the EMC[51] and SFM[52] groups on p and $\bar{p}$ fractions in quark jets. The enhancement of

Fig. 15:
Angular distribution of the $p\bar{p}$ system wrt the jet axis compared to the Lund (—) and Webber (--) model.

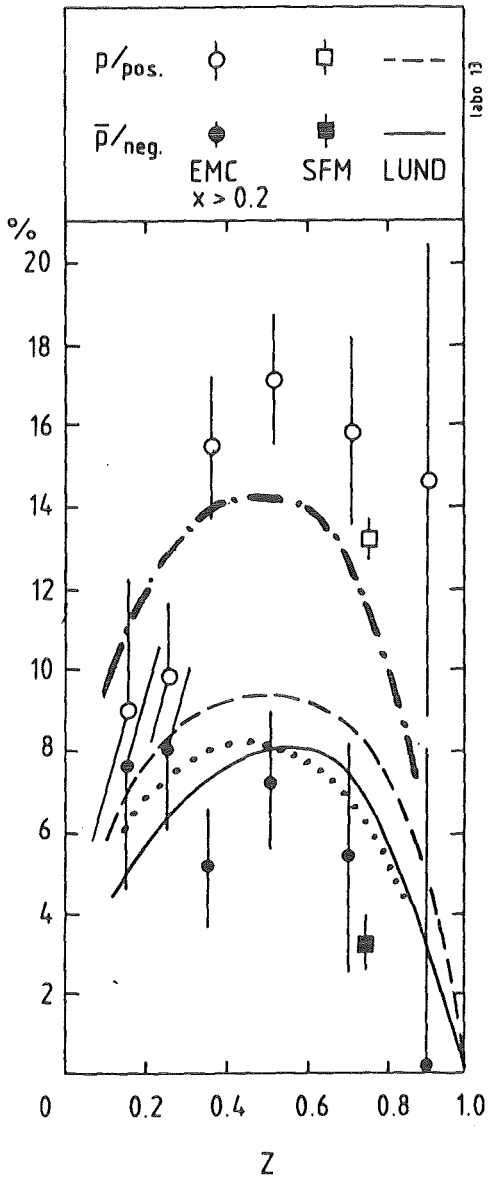

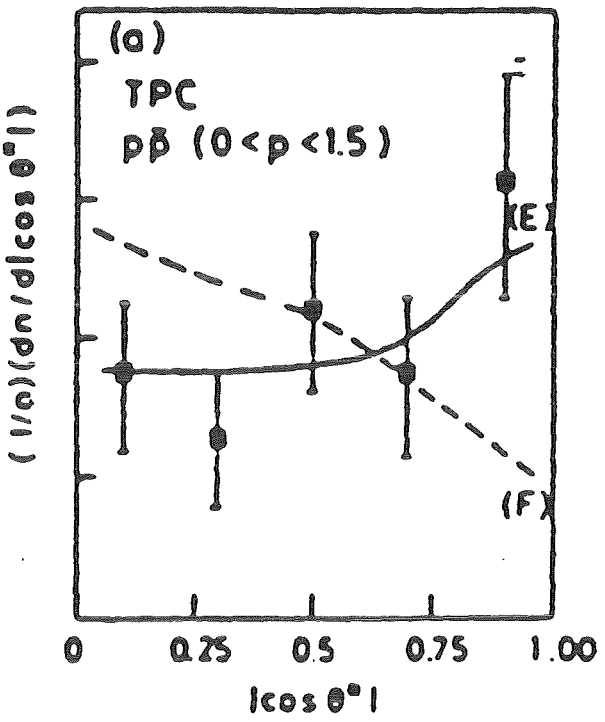

Fig. 16:
p,p̄ fractions in quark jets compared to a simple diquark (p--p̄——) and a popcorn model (p-·-p̄---).

p over $\bar{p}$ content of the jets (Fig. 16) cannot be explained by a simple diquark model, which would predict rather similar p and $\bar{p}$ fractions. If, however, 50% of 'popcorn' $B\bar{B}$ production is assumed and the diquark rate is increased from 0.065 to 0.1, the necessary enhancement of p's and suppression of $\bar{p}$'s can be obtained[45].

4. HEAVY QUARK FRAGMENTATION

It has been speculated quite early that heavy quark fragmentation should be harder than light quark fragmentation[53]. A parametrization based on simple phase space arguments has been suggested by Peterson et al.[54].

$$D(z) \sim 1/z \cdot (1 - 1/z - \varepsilon/1-z)^{-2}; \quad \varepsilon = (M_q/M_Q)^2 \qquad (8)$$

with the light and heavy quark masses M_q and M_Q. In the original work $\varepsilon_c \simeq 0.25$ and $\varepsilon_b \simeq 0.04$ were suggested.

To measure heavy quark fragmentation the c and b quark has to be tagged. Three methods have been used

a) direct reconstruction of leading charmed particles

b) decay of $D^* \to D\pi$

c) prompt leptons from charm and beauty decay.

Charm Fragmentation

I will first concentrate on a) and b) which give the most reliable results on charm fragmentation. D^0 and $D^{\pm}$ signals have been seen at the HRS[55] and CLEO[56] detector. Preliminary data are also available from the ARGUS collaboration[21]. The F meson has been seen by the CLEO[57], TASSO[58], HRS[59], and ARGUS[60] groups in the decay $F \to \phi\pi$, $\phi \to K^+K^-$, TASSO claims a significantly higher production rate than the other three experiments[3].

Three groups, ARGUS[66], JADE[64], and TPC [67], have searched for $F^* \to \gamma F$, $F \to K^+K^-\pi$. JADE has seen no signal, ARGUS claims a signal in the $F \to \phi\pi$ mode whereas the $KK\pi$ decay of TPC is not dominated by the $\phi\pi$ decay.

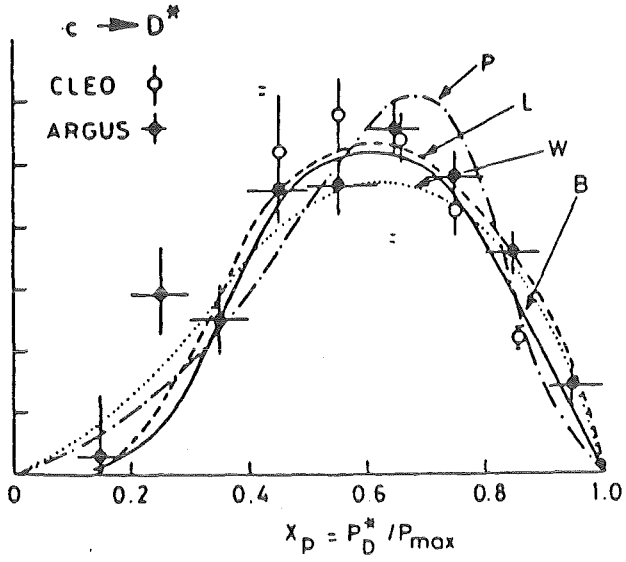

Fig. 17:
Charm fragmentation function (c → D*) compared to Bowler, Lund, Peterson, and Webber curves.

Method b) profits from the low Q values of the decay $D^* \to D\pi$. The low momentum of the $\pi^{\pm}$ can be measured with high precision. Thus the mass difference M(D*)-M(D) gives a much better constraint than the individual masses M(D*) and M(D). The method first applied by TASSO[61] has also been used by the ARGUS[21], CLEO[56], MARK II[63], HRS[63], JADE[64], and DELCO[65] groups.

Whereas all data agree quite well on the D and D* mesons, the situation is still unsatisfactory on the F mesons and in particular on the F*. (For recent reviews see ref 3, 4, and 68).

Fig. 17 shows[3] the charm fragmentation c → D* below beauty threshold obtained by the ARGUS[21] and CLEO[69] groups. Data are compared with the Peterson parametrization (8), the Lund and the Webber model. Also, a comparison is made with a function given by Bowler[16]

$$D(z) = (1-z)\, z^{-1} \exp\left[-bM_c^2 \frac{M_{D^*}^2}{M_c^2 z} - 1 - \ln \frac{M_{D^*}^2}{M_c^2 z}\right] \qquad (9)$$

which is based on the simple 'symmetric Lund' $(1-z)^{-1}z$ form used for light quarks (Table 1) modified by a tunneling factor.

All four models give a satisfactory fit to the data. The Peterson function requires a parameter $\varepsilon_{c\to D^*} = 0.15 \pm 0.01$ to fit the D* data of ARGUS[21]. The ARGUS parameter for D^0 fragmentation is $\varepsilon_{c\to D} = 0.25 \pm 0.02$ indicating that the D fragmentation is softer than D* fragmentation[21]. This can be explained by the observation that c

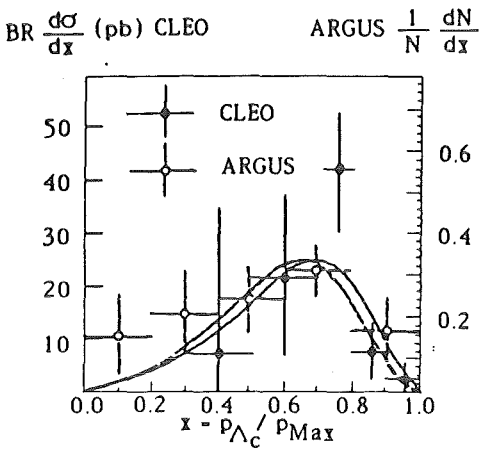

Fig. 18:
Charm fragmentation function ($c \rightarrow \Lambda_c$) compared to the Peterson function for two values of ε_c : 0.14 and 0.17.

fragmentation is dominated by D* production and the D's are mostly decay products of D*'s. The F, F* fragmentation appears to be even softer, with $\varepsilon_{c\rightarrow F,F^*} \simeq 0.4$ to 0.5.[21] This is again expected, since the heavier s quark has to be picked from the vacuum.

Λ_c production at 10 GeV e^+e^- interactions has been clearly established by the CLEO[69,70] and ARGUS[21] groups. The fragmentation functions measured by the two groups are shown[4] in Fig. 18. A fit using (8) yields $\varepsilon_{c\rightarrow\Lambda} = 0.172^{+0.128}_{-0.088}$ which is quite similar to the value found for D* fragmentation[4]. This supports the idea, that simple diquark fragmentation (c picks a diquark to produce Λ_c) is the dominating mechanism.

Another very interesting result on charm fragmentation comes from the ARGUS[21] group. They detected a new heavy charm meson in the decay chain

$$D^{**0}(\rightarrow 2420) \rightarrow D^{*+}\pi^- \quad ; \quad D^0 \rightarrow \quad K^-\pi^+$$
$$\hookrightarrow D^0\pi^+ \qquad\qquad K^-\pi^+\pi^-\pi^+$$
$$K^-\pi^+\pi^0$$

The group takes twice advantage of method b) and can extract a clear signal of 121^{+32}_{-21} events at a mass of (2420 ± 6 ± 6) MeV. A preliminary value for the fragmentation parameter is $\varepsilon_{c\rightarrow D^{**}} = 0.12 \pm 0.05$.

The yield of D** is $\sigma(D^{**})/\sigma(D^*) \gtrsim 0.24$. Since D^{**0} is most probably a p wave state, charm fragmentation has to include strong p wave contributions, which may be a strong challenge to fragmentation modelling (Fig. 19).

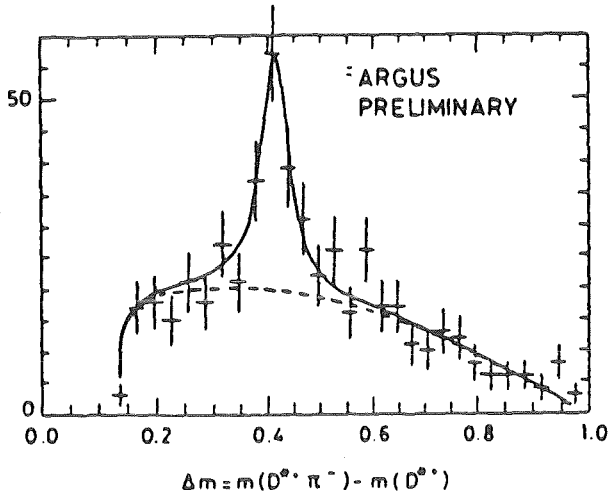

Fig. 19:
Signal of the D^{**0} in the mass difference $M(D^{*+}\pi^-) - M(D^{*+})$.

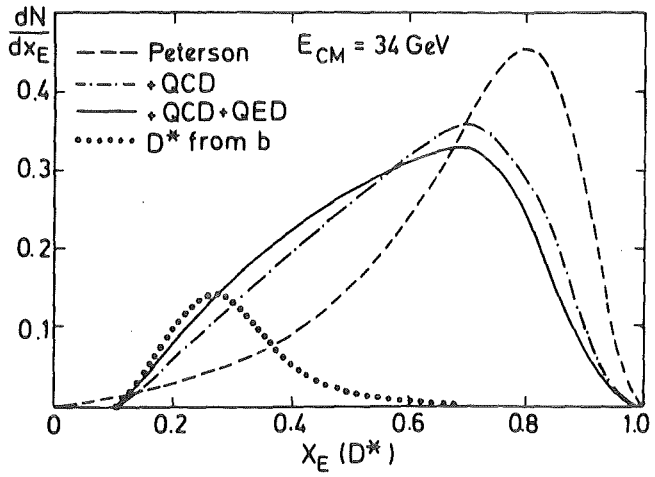

Fig. 20a:
Corrections to be applied to the measured fragmentation functions D(z).

The Peterson function (8) is derived for the light cone variable $z=(p_{||}+E)_h/(p_{||}+E)_Q$. Various corrections have to be applied to relate the theoretical $D_T(z)$ to the measured fragmentation functions $D_E(x)$ with $x = E_h/E_b$ or $x_p = p_h/p_b$. A recent assessment of the problem has been made by Bethke [71]. Fig. 20a shows the different ingredients to relate $D_T(z)$ and $D_E(x)$: QCD and QED (radiated gluons and photons) and background corrections for $b \to c$ decays. Fig. 20b gives the result for mean values of z before and after these corrections have been applied. After corrections good agreement of all measurements is found with a mean value of

$$\langle z_{c \to D^*} \rangle = 0.71 \pm 0.01 \pm 0.03$$

which corresponds to an ε_c significantly below the uncorrected value

$$\varepsilon_c \simeq 0.04.$$

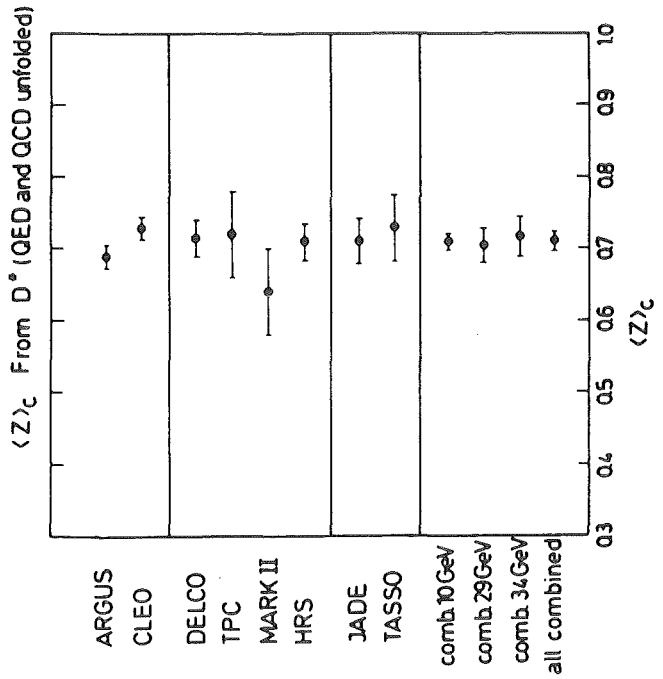

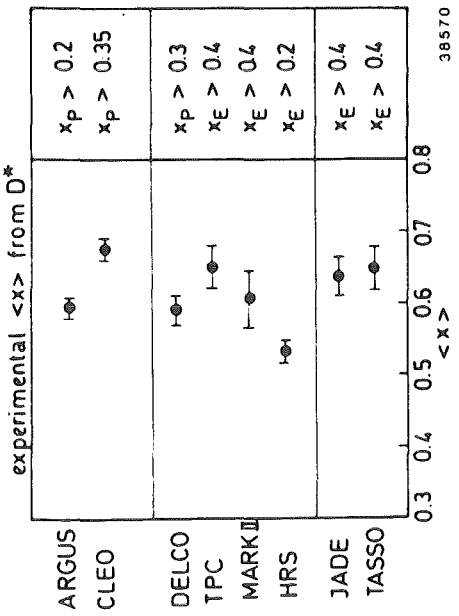

Fig. 20b:
Mean values of z before and after corrections.

Beauty Fragmentation

The only information on beauty fragmentation comes from the study of direct leptons (method c). Without going into any details I will just give one example of a fragmentation function obtained by the MARK J collaboration and a summary of the results[71] (Fig. 21)

$$\langle x_b \rangle = 0.80 \pm 0.03.$$

This value corresponds to a Peterson parameter (uncorrected) of

$$\varepsilon_b \simeq 0.01.$$

As expected, the b fragmentation is much harder than the c fragmentation. A nice consistency check can be obtained if one calculates M_q from ε_c and ε_b using relation (8):

$$M_q = 0.3 \text{ GeV} \quad (\varepsilon_c) \qquad \leftrightarrow \qquad M_q = 0.4 \text{ GeV} \quad (\varepsilon_b).$$

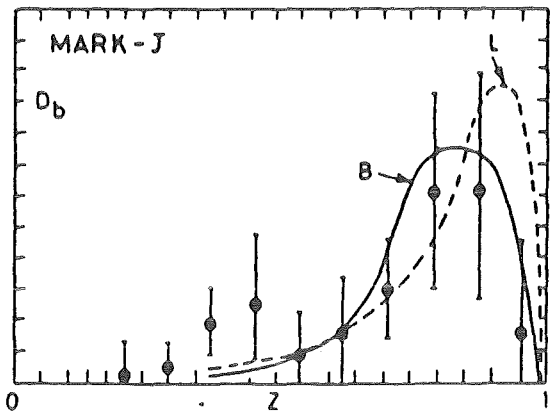

Fig. 21a:
Beauty fragmentation function derived from direct lepton data and

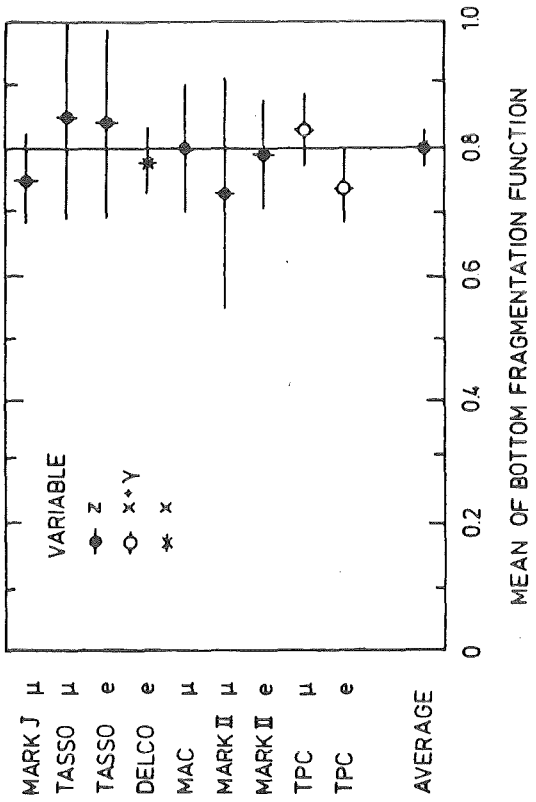

Fig. 21b:
Mean values of z (without correction).

5. GLUON FRAGMENTATION

5a. 'String Effect'

Not the concept of the fragmentation mechanism but rather the treatment of gluons turned out to be the decisive difference between IF and SF (Lund) models. If one studies the energy or particle flow in the event plane of 3-jet events the SF shows a relative depletion of particles between the two quark jets (Fig. 7a,b). This is due to the fact that the colour strings in which particles are produced are stretched between the quarks and the gluon ('string effect').

Experimentally the test is rather difficult, since the gluon jet has to be identified by the kinematics of the reaction $e^+e^- \rightarrow q\bar{q}g$. Choosing the lowest energy to tag the gluon gives an only 50% probability to really hit it. The effect has first been studied and established by the JADE group[72]. Their latest result is shown in Fig. 22. One can clearly see, that the depletion between the first

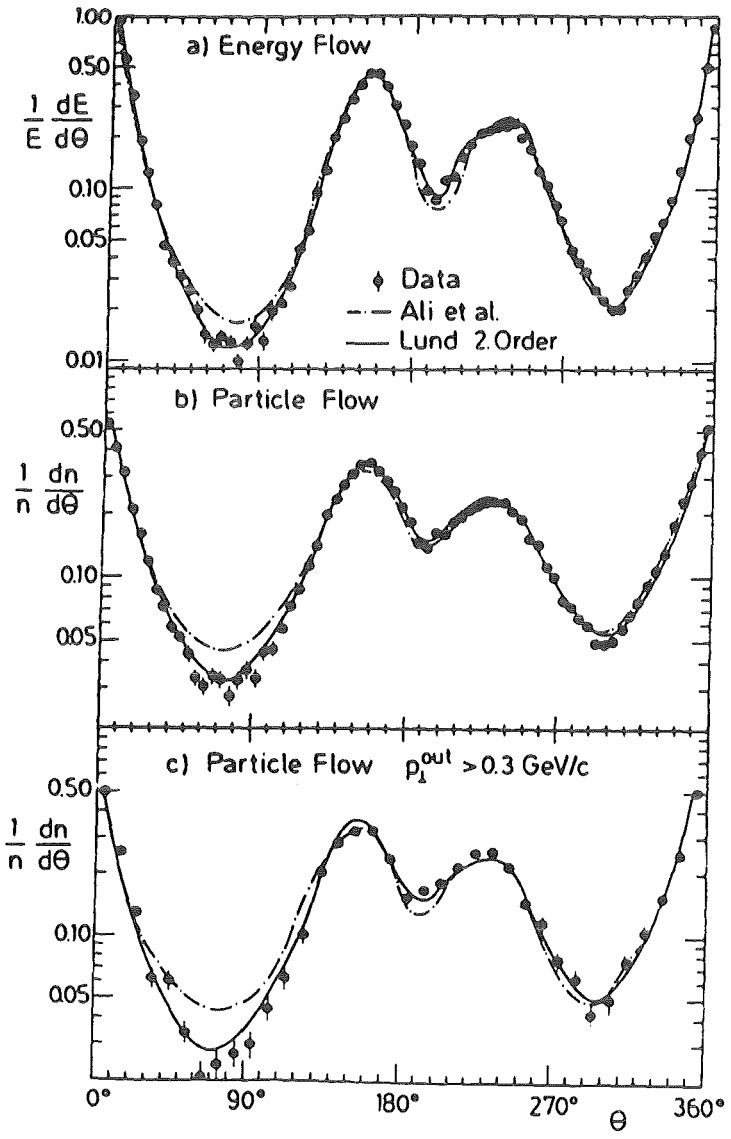

Fig. 22:
Energy and particle flow projected into the event plane compared to IF (Ali) and SF (Lund) model predictions.

('q') and the second ('g') jet can only be accounted for in the Lund model. The effect has been confirmed by the TPC[73], PLUTO[74], and TASSO[75] group and turns out to be the fatal blow for all IF models (Fig. 24).

Recently, the JADE collaboration extended their studies of the effect to QCD shower models (Fig. 23). Surprisingly enough it turned out that the Webber model again shows the effect, whereas the Gottschalk model does not[76]. The depletion between the quark jets is as well reproduced by the ordering of parton emission angles which results from the destructive interference in soft gluon emission taken into account in the Webber model.

Fig. 24 summarizes a comparison of different model predictions

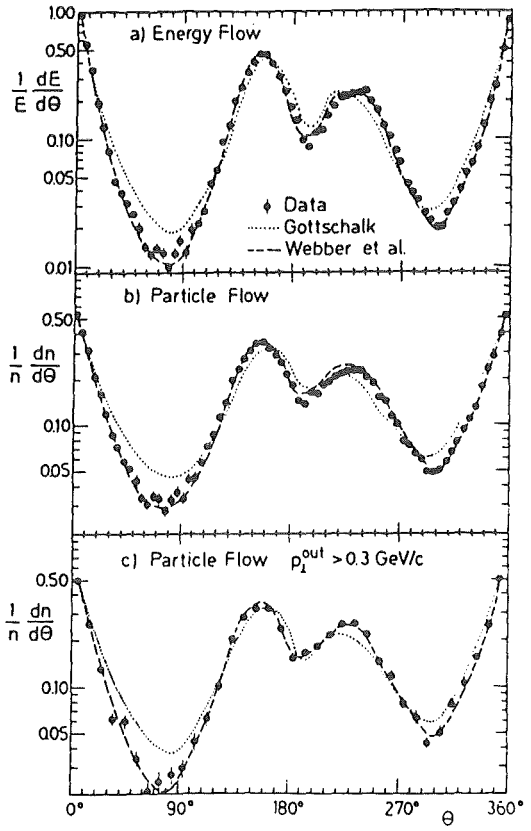

Fig. 23:
As Fig. 22, compared to two QCD shower models (Gottschalk and Webber).

with the measured ratio of particles between jet 1 and 3 ($q\bar{q}$) and jet 1 and 2 qg). Only the Webber and the Lund models survive.

5b. Difference Quark-Gluon Jets

Differences between quark and gluon fragmentation are expected due to the gluon selfcoupling. Asymptotically the colour factor 9/4 on the resulting three gluon vertex should be visible e.g. in the mean particle multiplicity (5). Consequentely, gluon fragmentation is expected to be softer than quark fragmentation.

Experiments so far have mostly been carried out at relatively low energies, showing little or no differences between quark and gluon fragmentation (e.g. in $\Upsilon \to 3g$ decay). Until recently JADE has been the only experiment claiming differences in the mean transverse momentum in $e^+e^- \to q\bar{q}g$.[77] Such measurements are difficult, because quark and gluon jets cannot easily be disentangled and they cover different energy ranges.

Recently, new data on this subject have become available from the UA1 collaboration[78]. Although the $\bar{p}p$ jet fragmentation is clearly softer than the one of e^+e^- and ISR jets, one should be careful in drawing quick conclusions about quark-gluon differences. The ISR and e^+e^- jet are produced at $Q^2 \lesssim 1000$ GeV^2 the $\bar{p}p$ jets however at $Q^2 \gtrsim 2000$ GeV^2. Thus at least a large portion of this difference could be due to scaling violation.

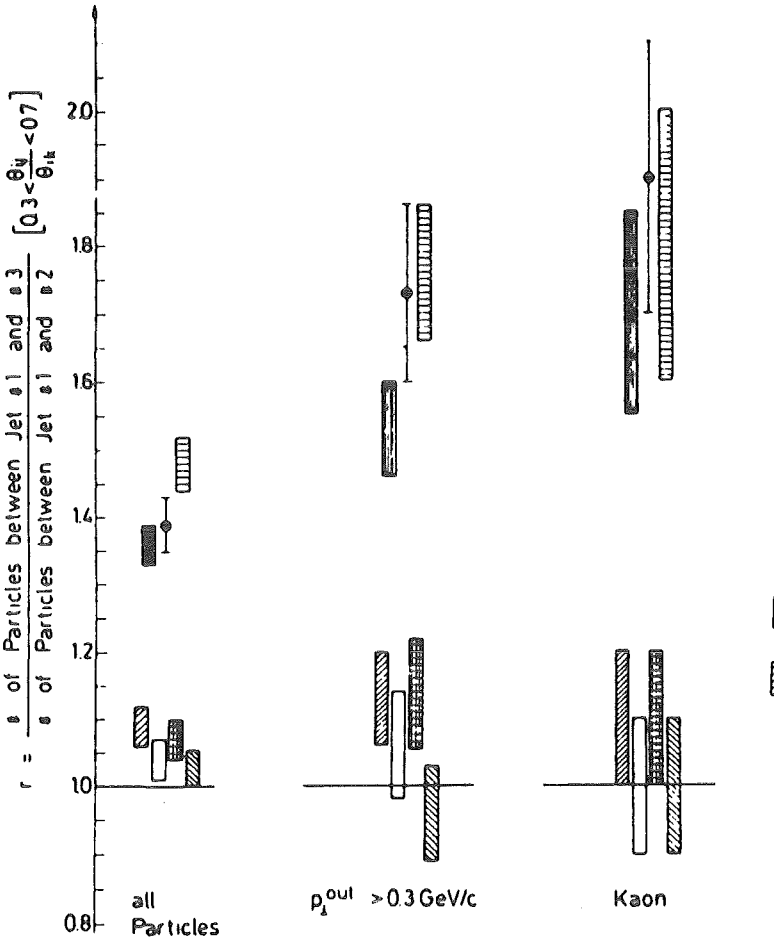

Fig. 24:
The ratio of number of particles between jets 1 and 3 ($q\bar{q}$) and 1 and 2 (qg) compared to different fragmentation models.

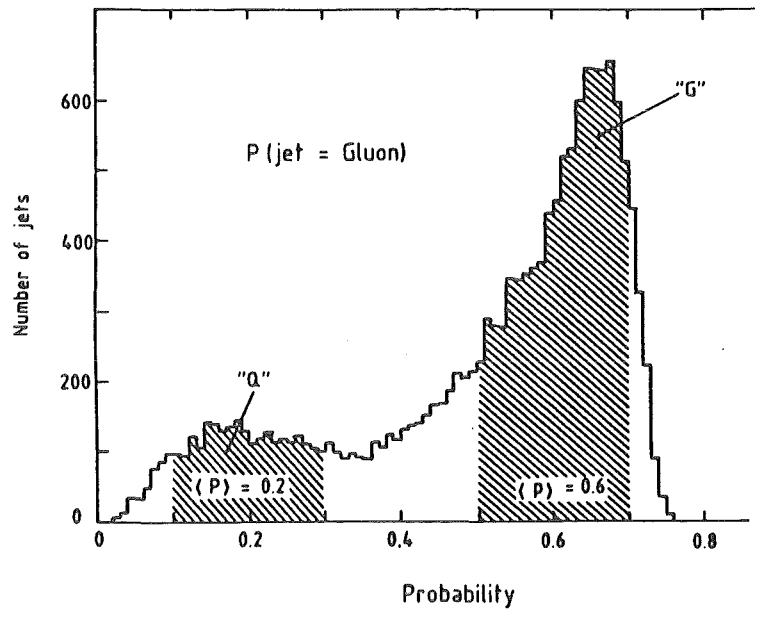

Fig. 25:
Probability of a jet being a gluon jet, Shaded areas are quark enriched 'Q' and gluon enriched 'G'.

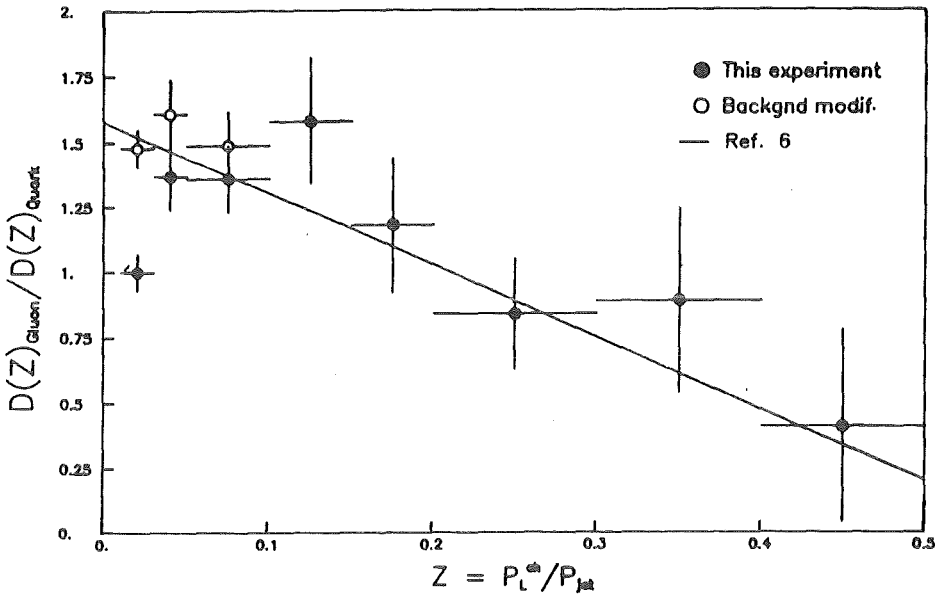

Fig. 26: Ratio of the gluon and quark fragmentation functions compared to a model prediction.

The UA1 collaboration therefore tried to disentangle quark and gluon jets in their data and thus compared them at similar high Q^2. They selected a clean two-jet event sample in which the full kinematic of the hard process can be reconstructed and the cross section

$$\sigma \sim F_1(x_1,Q^2)F_2(x_2,Q^2)\,\frac{d\hat{\sigma}}{d\hat{t}}\,(\cos\,\theta^*)$$

can be determined. They calculate cross sections σ under the assumptions that jet 1 and 2 are either quark or gluon jets, inserting the appropriate structure functions F_1, F_2 and the known hard scattering cross sections $\frac{d\hat{\sigma}}{d\hat{t}}\,(\cos\,\theta^*)$. Thus a probability can be determined for the jets being of quark or gluon origin. Fig. 25 shows the probability of a jet being a gluon. The two enhancements represent a quark enriched 'Q' and a gluon enriched 'G' sample of jets. 'Q' has a 83% probability of stemming from a quark jet, 'G' is 65% probably a gluon jet. The two fragmentation functions of these samples are compared in Fig. 26. Indeed, the ratio of the two fragmentation function shows that the gluon fragmentation is softer than the quark fragmentation. This conclusion however depends strongly on the treatment of background in the first few bins of the z distribution.

A nice consistency check between the low energy data and these results is contained in Fig. 27. It shows the Q^2 evaluation of the e^+e^- fragmentation function for different bins of z and its extrapolation to the $p\bar{p}$ Q^2 range. The quark fragmentation appears to follow this extrapolation quite well. The gluon sample however has a much softer fragmentation.

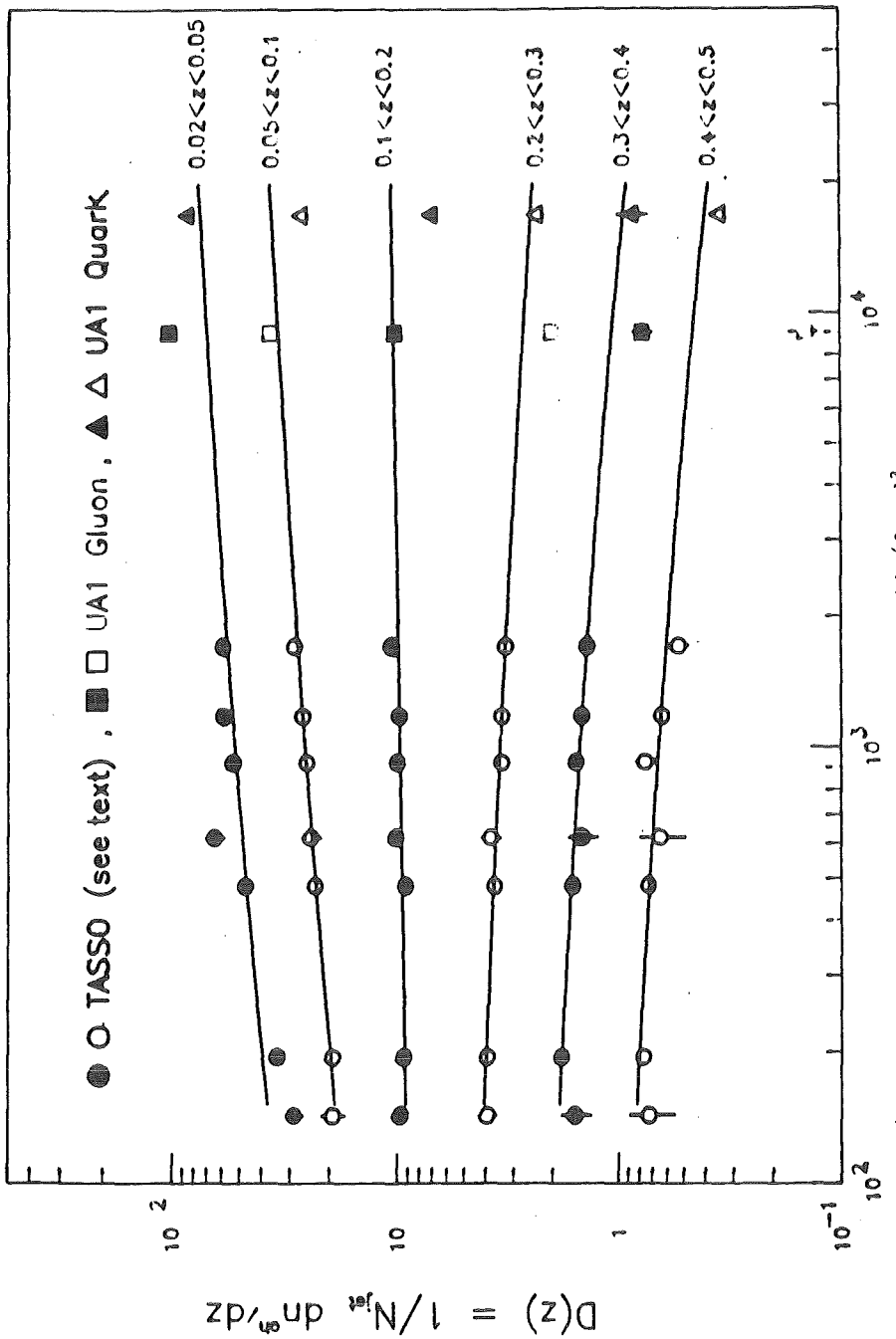

Fig. 27: Q^2 evolution of the mean quark fragmentation function in different z bins in e^+e^- annihilation extrapolated to the $S\bar{p}pS$ energy regime and compared with the 'Q' and 'G' data in the corresponding z bins.

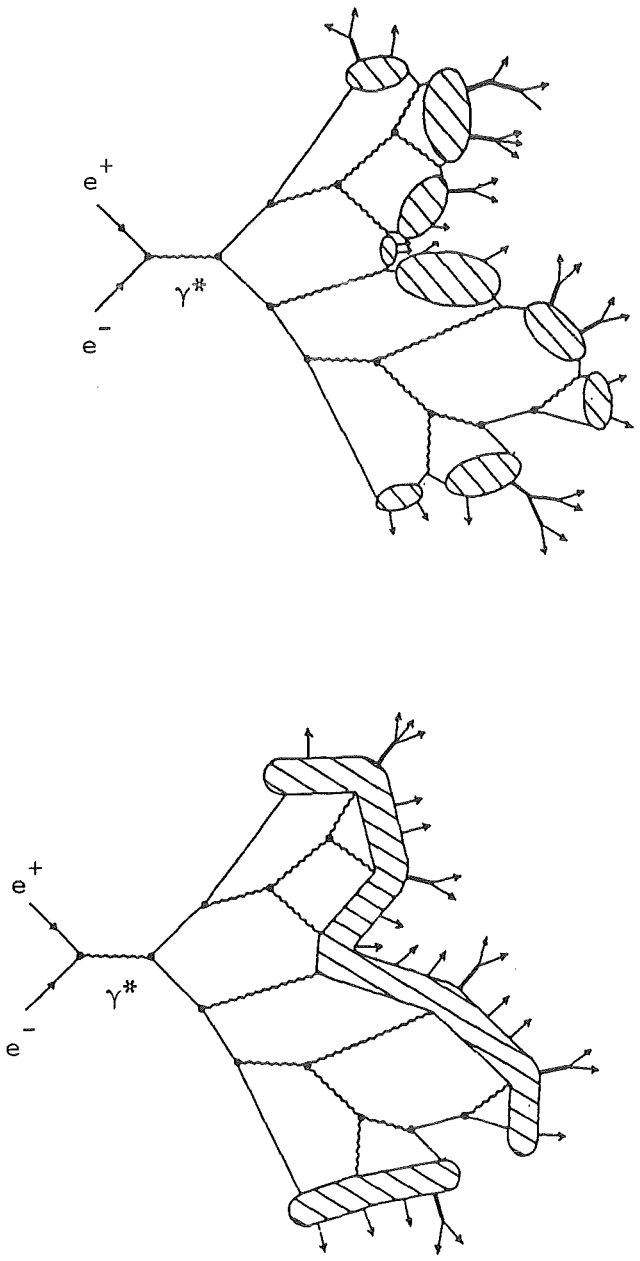

Fig. 28:
QCD shower model with cluster or string fragmentation.

The above analysis confirms (c.f. chapter 1b) that most (about 60%) of the jets in $\bar{p}p$ collisions stem from gluons. This result is also corraborated by the D* fragmentation function being much softer than in e^+e^- collisions[79]. The unexplainably large rate of D* production[80] seen by the UA1 group seems to be understood meanwhile as being due to normalization problems caused by the selection bias on the jets containing D*'s.[78]

6. CONCLUSION

In the last years we have seen an immense progress in understanding the large amount of data which is now available. There are essentially two models which are able to stand most of the tests: the string fragmentation (Lund) model and the QCD shower (Webber) model.

Both models are essentially able to describe the

- global jet distributions (multiplicities, inclusive spectra)
- particle content of jets (vector/pseudoscalar, strange particles)
- particle correlations (long range, short range)
- baryon production
- heavy quark fragmentation
- 'string effect'

However, both models also have their shortcomings.
The Webber model in its simple form does not correctly reproduce hard gluon bremsstrahlung, because the leading log approximation cannot give a good description at large Q^2. Thus the three jet rate and energy-energy correlations are not correctly reproduced. In addition, the final cluster decay gives wrong results in the high z inclusive spectra and in the angular correlations of baryon pairs.

The main adventage of the Webber model is of course that it is based on a QCD approach and that it makes do with so few parameters. Most of the shortcomings (except the hard gluon bremsstrahlung) seem to occur in the cluster decay at the end of the QCD cascade. It seems therefore quite natural to merge the two successful parts of the Lund and Webber model and terminate the QCD cascade by string fragmentation instead of cluster decay (Fig. 28). First attempts along these lines are underway[81].

ACKNOWLEDGEMENT

I am indebted to W.-D. Apel for critically reading and to V. Lallemand for carefully typing the manuscript.

REFERENCES

1) Di Lella, L., Int. Conf. on HEP, London, 1974, p. V-13
2) Hanson, G.G. et al., Phys.Rev.Lett. 35 (1975) 1609
3) Saxon, D.H., invited talk at the EPS Conference, Bari, 1985
4) Yamamoto, H., invited talk at the Int. Symp. on Lepton and Photon Interactions at High Energies, Kyoto, 1985
5) Mueller, A.H., invited talk at the Int. Symp. on Lepton and Photon Interactions at High Energies, Kyoto, 1985
6) Hollerbeck, R., SLAC Summer Institute on Particle Physics, Stanford, 1983, p. 53
Wolf, G., Int. Conf. on High Energy Physics, Paris, 1982, p. 525
Söding, P., Wolf, G., Am. Rev. Nucl. Part. Sci. 31 (1981) 231

7) Mueller, A.H., Nucl.Phys. B241 (1984) 141
Malaza E.D., and Webber, B.R., Phys.Lett. 149B (1984) 501 and
Cavendish preprint HEP 85/4 (1985)
Gaffney, J.B. and Mueller, A.H., Nucl.Phys. B250 (1985) 109
8) Dengler, F., proceedings of this conference
EMC Coll., Arneodo, M., preprint CERN-EP/85-26 (1985),
to be published in Nucl.Phys.B
9) Ekspong, G., proceedingsof this conference
10) TASSO Coll., Althoff, M. et al., DESY 85-077 (1985)
11) HRS Coll., Derrick, M. et al., preprint ANL-HEP-CP-85-60, 1985
12) Uhlig, S. et al., Nucl.Phys. B132 (1978) 15
UA5 Coll., Alpgard, K. et al., Phys.Lett. 123B (1983) 361
13) Hofmann, W., Symp. on High Energy e^+e^- Interactions,
Nashville, 1984
14) Field R.D. and Feynman R.P., Nucl.Phys. B136 (1978) 1
Hoyer, P., et al., Nucl.Phys. B161 (1979) 349
Ali, A. et al., Phys.Lett. 93B (1980) 155
Meyer, T., Z. Physik C12 (1982) 77
15) Artru, X. and Mennessier, G., Nucl.Phys. B70 (1974) 93
16) Bowler, M.G., Z. Physik C11 (1981) 169, C22 (1984) 155
17) Anderson, B. et al., Z. Physik C20 (1983) 317,
Phys.Rep. 97 (1983) 33
18) Bassetto, A. et al., Nucl.Phys. B163 (1980) 477
Marchesini, G. et al., Nucl.Phys. B181 (1981) 335
Marchesini, G., XV Int. Symp. on Multip. Dynamics, Lund, 1984,
with further references
19) Gottschalk, T.D., Nucl.Phys. B214 (1983) 201
20) Webber, B.R., Nucl.Phys. B238 (1984) 492 and
XV Int. Symp. on Multip. Dynamics, Lund, 1984
21) Albrecht, H., proceedings of this conference
22) HRS Coll., Derrick, M. et al., preprint ANL-HEP-CP-85-45 (1985)
23) ARGUS Coll., Albrecht, H. et al., Phys.Lett. 157B (1985) 326
24) JADE Coll., Bartel, W. et al., DESY 85-081 (1985)
25) CLEO Coll., Behrends, S. et al., Phys.Rev. D31 (1985) 2161
26) HRS Coll., Derrick, M. et al., preprint ANL-HEP-CP-85-69 (1985)
and contribution to the EPS Conference, Bari, 1985
27) Oddone, P., SLAC Summer Institute on Particle Physics,
Stanford, 1984
28) Barbaro-Galtieri, A., XV Symp. on Multip. Dynamcis, Lund, 1984
29) Hofmann, W., Int. Symp. on Multip. Dynamics, Kiryat-Anavin, 1985
30) TASSO Coll., Althoff, M. et al., Phys.Lett. 100B (1981) 357 and
DESY 85-077 (1985)
31) PLUTO Coll., Berger, Ch. et al., Nucl.Phys. B214 (1983) 189
32) TPC Coll., Aihara, H. et al., Phys.Rev.Lett. 53 (1984) 2199
33) Goldhaber, G. et al., Phys.Rev. 120 (1960) 300
34) Goldhaber, G., Int. Conf. on HEP, Lisbon, 1981, p. 767
35) TPC Coll., Aihara, H. et al., Phys.Rev. D31 (1985) 996
36) CLEO Coll., Avery, P. et al., preprint CLNS-85/649 (1985)
37) AFS Coll., Akesson, T. et al., Phys.Lett. 129B (1983) 269 and
155B (1985) 128

38) Bell, K.W. et al., Rutherford RAL-82-011 (1982)
39) Cerny, V. et al., Phys.Rev. D16 (1977) 2822, D18 (1978) 2409
40) Meyer, T., Z. Physik C12 (1982) 77
41) Ekelin, S. et al., Phys.Rev. D30 (1984) 2310
42) Anderson, B. et al., Nucl.Phys. B197 (1982) 45
43) Bartl, A. et al., Z. Phys. C20 (1983) 263,
Phys.Lett. 122B (1983) 427
44) Ingelmann, G., XV Symp. on Multip. Dynamcis, Lund, 1984
45) Anderson, B. et al., Lund Report LU TP 84-9 (1984)
46) Field, R.D., Phys.Lett. 135B (1984) 203
47) TASSO Coll., Althoff, M. et al., Z. Physik C17 (1983) 5
48) TPC Coll., Aihara, H. et al., Phys.Rev.Lett. 52 (1984) 2201
49) TASSO Coll., Althoff, M. et al., Phys.Lett. 139B (1984) 126
50) TPC Coll., Aihara, H. et al., Phys.Rev.Lett. 55 (1985) 1047
51) EMC Coll., Aubert, J.J. et al., Phys.Lett. 103B (1981) 388,
Phys.Lett. 135B (1984) 225
52) SFM Coll., Breakstone, A. et al., CERN/EP 85-30 (1985)
53) Bjorken, J.D., Phys.Rev. D17 (1978) 171
Suzuki, M., Phys.Lett. 71B (1977) 139
54) Peterson, C. et al., Phys.Rev. D27 (1983) 105
55) HRS Coll., Derrick, M. et al., Phys.Rev.Lett. 53 (1984) 1971
56) CLEO Coll., Bebek, C. et al., Phys.Rev.Lett. 49 (1982) 430,
Avery, P. et al., Phys.Rev.Lett. 51 (1983) 1139
57) CLEO Coll., Chen, A. et al., Phys.Rev.Lett. 51 (1983) 634
58) TASSO Coll., Althoff, M. et al., Phys.Lett. 136B (1984) 139
59) HRS Coll., Derrick, M. et al., Phys.Rev.Lett. 54 (1985) 2568
60) ARGUS Coll., Albrecht, H. et al., Phys.Lett. 153B (1985) 343
61) TASSO Coll., Althoff, M. et al., Phys.Lett. 126B (1983) 493
62) MARK II Coll., Yelton, J.M. et al., Phys.Rev.Lett. 49 (1982) 430
63) HRS Coll., Derrick, M. et al., Phys.Lett. 146B (1984) 261
64) JADE Coll., Bartel, W. et al., Phys.Lett. 146B (1984) 121 and
DESY 85-069 (1985)
65) DELCO Coll., Yamamoto, H. et al., Phys.Rev.Lett. 54 (1985) 522
66) ARGUS Coll., Albrecht, H. et al., DESY 84-052 (1984)
67) TPC Coll., Aihara, H. et al., Phys.Rev.Lett. 53 (1984) 2465
68) Izen, J.M., XV Int. Symp. on Multip. Dynamics, Lund, 1984
69) Galik, R., EPS conference, Bari, 1985
70) CLEO Coll., Bowcock, T. et al., Phys.Rev.Lett. 55 (1985) 923
71) Bethke, S., DESY 85-067 (1985)
72) JADE Coll., Bartel, W. et al., Phys.Lett. 101B (1981) 129,
134B (1984) 275
73) TPC Coll., Aihara, H. et al., Phys.Rev.Lett. 54 (1985) 270
Z. Phys. C28 (1985) 31
74) Maxeiner, H., PhD Thesis, Hamburg, 1984 (unpublished)
75) TASSO Coll., Althoff, M. et al., DESY 85-063 (1985)
76) JADE Coll., Bartel, W. et al., Phys.Lett. 157B (1985) 340
77) JADE Coll., Bartel, W. et al., Phys.Lett. 123B (1983) 460
Z. Phys. C21 (1983) 144
78) Ghez, P. proceedings of this conference
79) UA1 Coll., Arnison, G. et al., Phys.Lett. 147B (1984) 222
80) Ali, A. and Ingelman, G., CERN-TH 4105/85 (1985)
81) Ingelman, G., CERN-TH 3969 (1984)